Progress In Electromagnetics Research B, Vol. 27, 235–251, 2011

WIDE BEAM TAPERED SLOT ANTENNA FOR WIDE ANGLE SCANNING PHASED ARRAY ANTENNA

A. Kedar and K. S. Beenamole

Electronics & Radar Development Establishment (LRDE)
C V Raman Nagar, Bangalore 560093, India

Abstract—Design and development of a low profile, compact, wide beam and wide band printed double layered exponentially tapered slot antenna (DTSA) with a coplanar waveguide (CPW) feed meant for wide scan active phased array antenna in X-band has been presented. DTSA satisfies the requirements on the maximum reflection coefficient of $\Gamma \leq -10\,\text{dB}$ for $\pm 60^\circ$ and $\pm 45^\circ$ scan from broadside in H- and E-planes, respectively with a moderate gain of 4–7 dBi. Realized antenna has shown a symmetric pattern together with moderately high gain, low cross-polarization and 3 dB beam width better than $\pm 60^\circ$ and $\pm 45^\circ$ in H- and E- planes, respectively. The designed structure is expected to find applications in mounting platforms with limited RF real estate available to it like in military aircrafts, owing to its easy integration with the uni-planar monolithic millimeter-wave integrated circuits.

1. INTRODUCTION

State of the art these days is multifunctional active electronically scanned arrays (AESA) offering numerous advantages; extremely fast scanning rate giving low probability of interception (LPI) features, higher ranges, beam agility, enhanced performance and functionality, increased ECCM resistance and high effective radiated power (ERP) [1]. Fighter radars have to detect targets in heavy clutter and dense jammer conditions, which means that near and far side lobes must be very low [2, 3]. AESA requires active phased array antenna elements employing wide band and wide beam antenna elements like dipoles, open-ended waveguides, slotted waveguide, microstrip antenna, helices and spiral antenna etc., as array elements to achieve

Received 5 October 2010, Accepted 3 December 2010, Scheduled 10 December 2010
Corresponding author: Ashutosh Kedar (ashutosh.kedar@gmail.com).

above-mentioned features [4–7]. The shape and direction of the beam is determined by the relative phases and the amplitudes applied to each radiating elements [6–9].

The modern shared aperture radar concept explored the development of multi function wideband arrays capable of simultaneous and time interleaving, electronic warfare, and communications functions [2, 3]. This necessitated the need of frequency independent wide band antennas [5, 7]. With the term frequency independent it is meant that the antenna pattern and impedance remain constant over a relatively wide frequency bandwidth.

Tapered slot antenna (TSA), also known as flared notch or Vivaldi antenna, is among one of the most promising candidate satisfying all requirements described above. TSA has the unique characteristics of symmetrical patterns in two planes, high gain (7–10 dB) in addition to having wide bandwidth characteristics in terms of radiation performance and impedance characteristics. The traits of TSA have been explored by many researchers, the references being mentioned by K. Chang in his editorial work [6]. TSA has a slotline flare from a small gap (50 Ω) to a large opening, matching to free space's wave impedance of 377 Ω and is usually parasitically fed by a "hockey-stick" balun at the base of the element [6, 10]. TSA is usually larger than a half wavelength to achieve the desired performance that increases the size of the array which poses certain restrictions in its installation on military platforms with limited real estate for RF front ends. This demands a reduction in size of the structure without sacrificing the performance advantages of a TSA. Lots of researchers have presented miniaturized compact designs of TSAs [6, 11, 12]. An attempt to achieve one such compact TSA design for airborne radar applications has been made in this paper for readers' reference.

This paper describes design and development of a compact, wide band and wide beam double layered exponentially tapered slot antenna (DTSA) fed by a coplanar waveguide (CPW) feed to facilitate its integration with uni-planar MMICs. The complete design and optimization of the antenna has been done using a general purpose commercial Finite Element based electromagnetic simulator (EM), HFSS [13]. The design has been done while considering the element performance in the array environment taking into account the effect of neighboring array elements on its performance, which is very essential to establish the suitability of the array element for its usage in active phased arrays [4–9, 14–17]. Further sections presented below discuss the design, fabrication and various results of simulation and measurements.

2. REQUIREMENTS AND GOALS

The phased array antenna is assumed to be very large so that the central elements can be approximated by an element in an array antenna of an infinite extent [8, 9, 14–17]. This simplifies the design since only a single unit cell with periodic boundaries needs to be considered [8, 9]. The element is designed to operate over full X-band defined by the requirement on the maximum reflection coefficient of $\Gamma \leq -10\,\text{dB}$ for $\pm 60^\circ$ and $\pm 45^\circ$ scan from broadside in H- and E-planes, respectively with a moderate gain of 4–7 dB over this band. Further, element was required to be compact so that it does not increase the depth of the overall active phased array unit, as it is meant to be used in airborne applications.

3. ELEMENT DESIGN

The design parameters of a doubly layered exponentially Tapered Slot Antenna (DTSA) are defined in Figures 1 and 2. Figure 1(a) illustrates the commercially available electromagnetic simulator HFSS model of the proposed geometry of DTSA. It consists of a section of slotline that is narrow at one end and has opening in an exponential flare at the other end. The antenna geometry can be classified into two categories: *substrate parameters* (relative dielectric constant, ε_r, and thickness, $h_s = t/2$) and *antenna element parameters* which can be sub-divided into the stripline/slotline transition, stripline/CPW transition, the tapered slot, stripline and slotline cavity, see Figure 1(a) (insets in the figure shows the stripline feed along with the via and the front view of the via).

The model illustrates two substrates back to back consisting of radiating flare geometries on the two opposite faces. One of the substrate is etched completely on the opposite side of the flare and the other substrate consists of stripline line feed being printed and sandwiched between the two substrates containing the flares. Figure 1(b) shows the schematics of the three layers forming the complete antenna assembly viz., namely; bottom patch; top patch and the middle layer (stripline feed). DTSA has been fabricated using printed circuit processing techniques on a Cuclad dielectric substrate (e.g., RT-Duroid). The flares acts as an impedance transformation network between free space and the stripline feed. Radiation from the antenna occurs when the slotline impedance is matched to the impedance of free space. The structure has self-scaling property as each portion of it corresponds to a narrow frequency spectrum of the whole designated frequency range of operation. Figure 2 shows

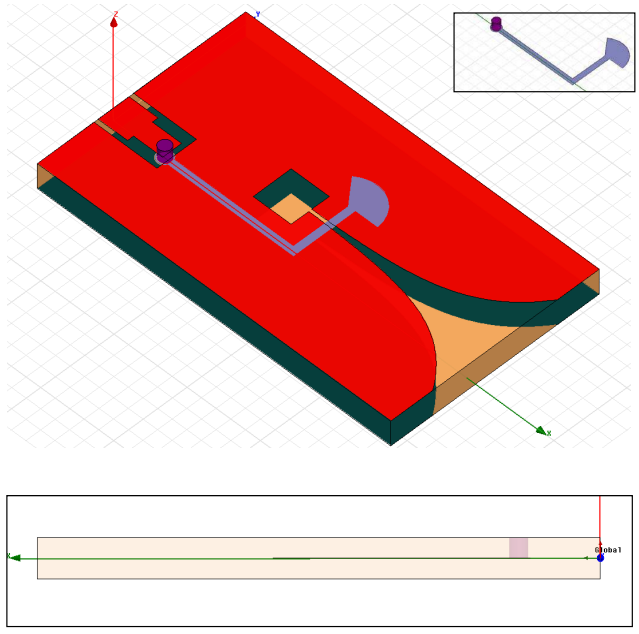

(a)

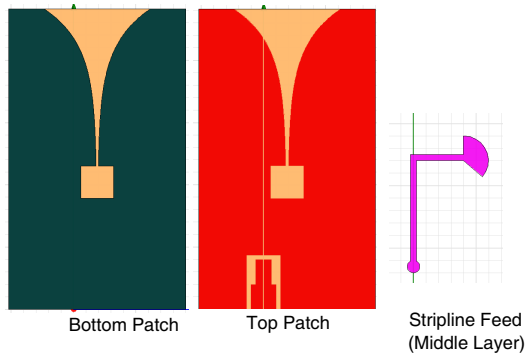

(b)

Figure 1. (a) Schematic of the tapered slot antenna geometry illustrating full assembly and the details of the various parts involved in the design. (As an inset are shown stripline feed and the front view of via for realizing the stripline-to-CPW transition). (b) Shown are the schematics of top, bottom and the middle layers of the antenna assembly.

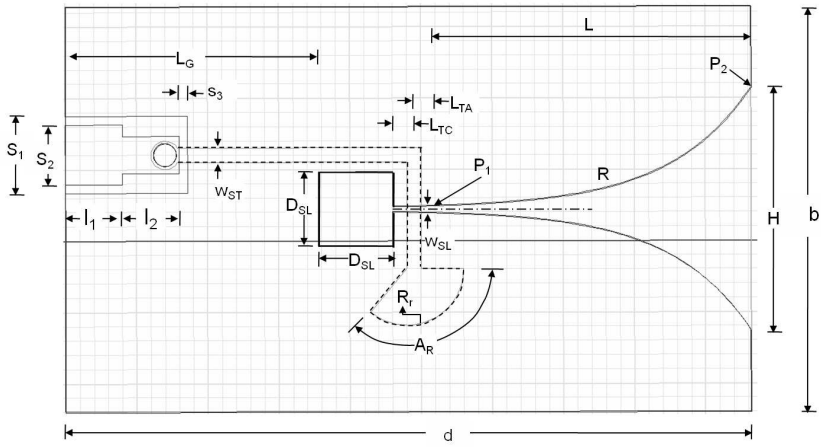

(a)

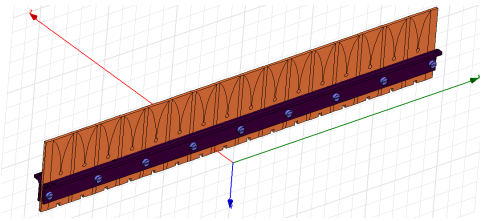

(b)

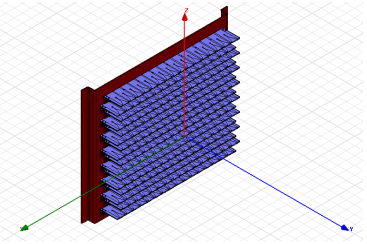

(c)

Figure 2. (a) Sketch of the tapered slot antenna geometry showing design parameters' details. Dimensions (all in mm): $H = 8.5$; $b = 14.2$; $d = 24.1$; $L = 11.6$; $R = 0.35$; $A_R = -130$ deg; $R_r = 2.02$; $D_{SL} = 2.6$; $W_{SL} = 0.2$; $W_{ST} = 0.5$; $S_1 = 2.7$; $S_2 = 2.1$; $S_3 = 0.7$; $l_1 = l_2 = 2$; $L_{TC} = 0.74$; $L_{TA} = 0.74$; $L_G = 8.9$. (b) Model of 1-D E-plane antenna array as modeled in HFSS. (c) Model of 2-D antenna array as modeled in HFSS.

the detailed sketch of the optimised geometry and the transition with various respective design parameters' details.

The stripline/slotline transition is specified by W_{ST} (stripline width) and W_{SL} (slotline width). The exponential taper profile is defined by the opening rate R and two points $P_1(x_1, y_1)$ and $P_2(x_2, y_2)$ (axis of the antenna is along the x-axis, see Figure 1(a)) [15]

$$y = c_1 e^{Rx} + c_2 \tag{1}$$

where

$$c_1 = \frac{y_2 - y_1}{e^{Rx_2} - e^{Rx_1}}$$

and

$$c_2 = \frac{y_1 e^{Rx_2} - y_2 e^{Rx_1}}{e^{Rx_2} - e^{Rx_1}}$$

The taper length, L is $x_2 - x_1$ and the aperture height is H is $2(y_2 - y_1) + W_{SL}$. In the limiting case where R approaches zero, the exponential taper results in a so-called linearly tapered slot antenna (LTSA) for which the taper slope is constant and given by $s_0 = (y_2 - y_1)/(x_2 - x_1)$. For the exponential taper defined by Eq. (1), the taper slope, s changes continuously from s_1 to s_2, where s_1 and s_2 are the taper slopes at $z = z_1$ and at $z = z_2$, respectively, and $s_1 < s < s_2$ for $R > 0$. The taper flare angle is defined by $\alpha = \tan^{-1} s$. The flare angles, however, are interrelated with and defined through other parameters, i.e., H, L, R and W_{SL}.

Design process of the DTSA involves the solution of three matching problems, one associated with the stripline-to-slotline feed transition; second is stripline/CPW transition and third and final associated with the notch-to-free space transition. The stripline-to-slotline transition has been designed using a radial stub and a square stub as shown in Figure 1 to achieve impedance match over the desired frequency band. CPW-to-stripline transition has been designed using a via and is optimized for wide bandwidth facilitating interconnection of the element with uni-planar MMICs. Notch to free space transition has been optimised by varying flare parameters; R, H and b. In our design, we achieved good results applying a combination of simple equivalent circuit models [10, 15, 18–20] and optimization using finite-element based general purpose commercial EM software, HFSS [13].

The parameters related to the stripline stub and slotline cavity shown in Figure 2 are as follows:

R_r radius of radial stripline stub;

A_R angle of radial stripline stub;

D_{SL} edge length of square slotline cavity;

L_G offset of slotline cavity from the ground plane;

L_{TC} distance from the transition to the slotline cavity;

L_{TA} distance from the transition to the taper.

Figure 2(a) shows the detailed design parameters of DTSA being considered in modelling the DTSA using HFSS and Figures 2(b) and 2(c) show the HFSS models of 1-dimensional E-plane antenna array with element arranged in a linear grid with E-plane spacing, dx

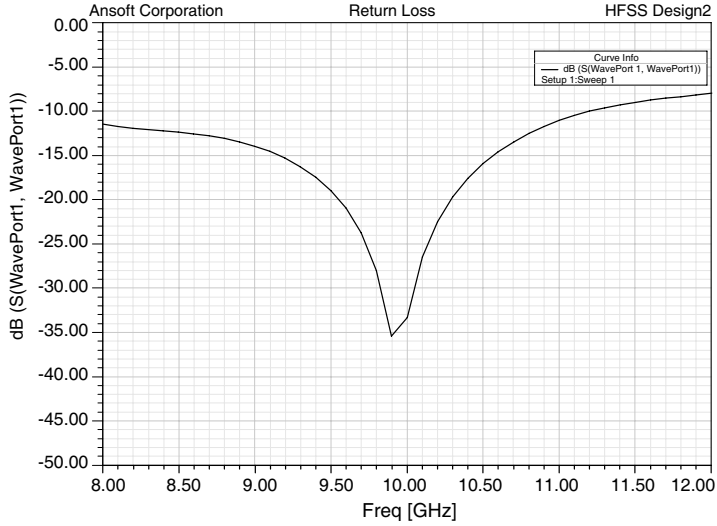

Figure 3. Simulated return loss versus frequency plot of DTSA.

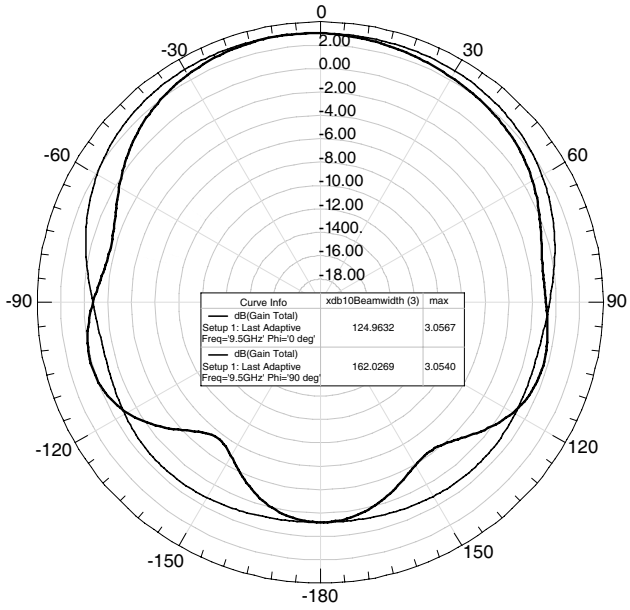

Figure 4. Simulated radiation pattern plot of DTSA in two principal planes.

and 2-dimensional planar array with H-plane spacing, dy, at centre frequency, f_0, respectively. The respective grid spacings have been chosen to avoid onset of the grating lobes at the higher operating frequency in the visible region. The RF connectors used for feeding are SMP series connectors from Radiall Inc. The optimization of DTSA has been done using HFSS in array environment and all the optimized dimensions (in mm) have been shown in Figure 2(a). The detail of the embedded element performance is being discussed in the next section.

Figure 3 shows the simulated return loss (RL) plot of isolated DTSA element showing the achieved $RL < -10\,\text{dB}$ over the desired frequency band. Figure 4 shows the simulated radiation pattern plots in H- and E-planes, respectively of isolated DTSA element illustrating the achieved 3 dB beamwidth (HPBW) greater than $\pm 60^\circ$ in the two respective planes as desired.

4. EMBEDDED ELEMENT PERFORMANCE

Array performance strongly depends on the coupling in a wide bandwidth and wide scanning arrays. So the mutual coupling study is extremely important in the design process of an active phased array. Analysis of antenna array is limited by computer memory resources. Assuming large periodic arrays with a substantial number of elements so that edge effects are negligible, many of the numerical array analyses are efficiently conducted on a unit cell of the array using periodic boundary conditions [8, 9]. Periodic boundary conditions, which simulate an infinite array are satisfied either through the summation of *Floquet* modes or through numerical waveguide simulators [9].

4.1. Mutual Coupling

The linear array antenna is assumed to be consisting of K identical elements, displaced a distance, d, with respect to one another and being matched to a voltage source as shown in Figure 5 [9]. Since the radiators are match-connected to their sources, the voltage waves traveling in negative directions are only due to mutual coupling from surroundings. To obtain the *scan element pattern (SEP)*, only one of the K elements will be excited, the other elements will be disconnected from their sources and will be terminated in matched (reflection less) loads. This situation is shown for element k, where $k = 1, 2, \ldots, K$, in Figure 5(a). The effect of the mutual coupling is shown in Figure 5(b) by the presence of waves traveling from the not-excited elements into the loads.

The K-element linear array may be seen as a K-port,

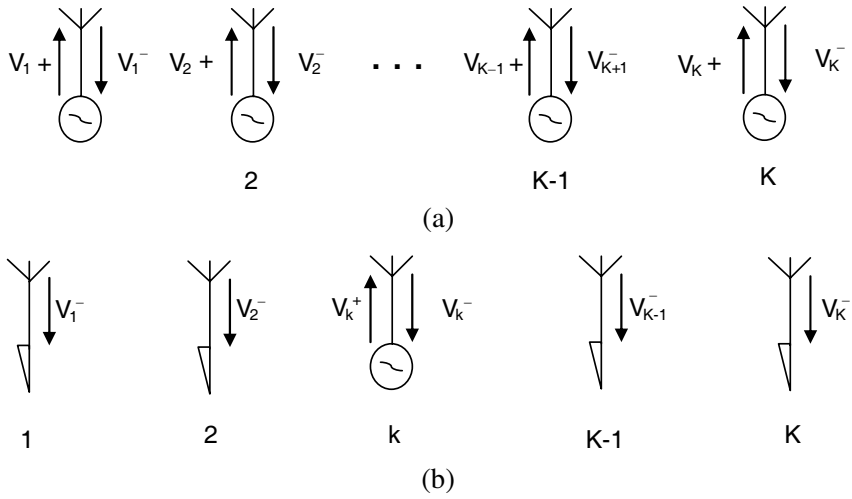

Figure 5. K-element linear array antenna. (a) Every element is match-connected to a voltage source. (b) Feeding for obtaining the scan element pattern for element k.

characterized by a $K \times K$ scattering matrix, where the scattering coefficients relate the element voltage wave amplitudes according to $S_{kl} = V_k/V_l^+$, which is obtained by comparing the voltage wave amplitude of the wave entering element k from free space with the voltage wave amplitude of the wave exciting element l. For this comparison, none of the elements, with the exception of element l is being excited. All these elements are terminated in matched load. For a uniformly-lit, K-element linear array, the active reflection coefficient of an element with index m is given as [9].

$$\Gamma_m(\theta_0) = \Sigma_{n=1}^{K} S_{mn} e^{-jknds\sin\theta_0} \tag{2}$$

In Eq. (2), S_{mn} are the n-port scattering parameters of the array, k is the free space wave number, dx is the linear spacing between elements, and θ_0 is the scan angle.

Scan element pattern (SEP) is the radiation pattern of a singly excited element in its array environment where all other elements are terminated into matched loads. SEP will provide the phased array antenna gain at the position of the scanned beam as a function of scan angle. For a large phased array antenna, all SEP will be nearly identical and hence, the phased array antenna performance may be approximated by applying pattern multiplication-scan element pattern is multiplied with the array factor. All coupling effects are accounted for in the scan element pattern [8, 9].

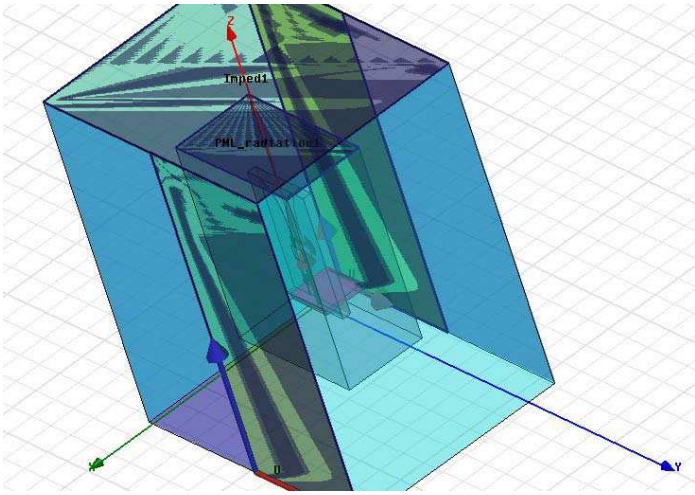

(a)

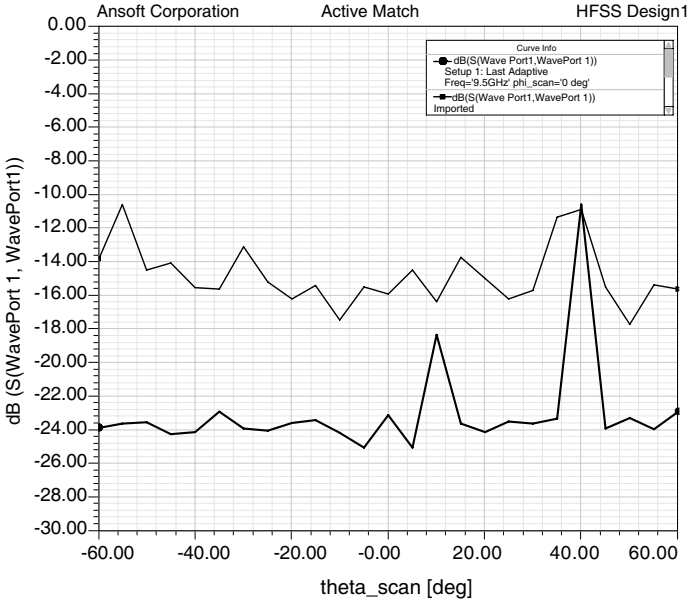

(b)

Figure 6. (a) Unit cell model of the DTSA as modeled in HFSS. (b) Simulated active reflection coefficient of DTSA in (i) H-plane (solid line). (ii) E-plane (dotted line).

The measurement of mutual coupling makes it easier to predict the scan performance of the array. Another way to analyze the scan performance is by using *Floquet* modes and the unit cell approach where infinite array is emulated by enclosing the antenna element by electric/magnetic walls which act like mirror walls showing infinite elements on either side of the grid along x- or y-directions (see Figure 6(a)) [21]. The reference [21] clearly describes the methodology of applying HFSS software in analyzing the performance of antenna element in infinite array environment for rectangular and triangular lattice arrangements. The same technique is incorporated in the present work to analyze the element performance in the array environment.

4.2. Simulations

An array of 16×16 elements (see Figure 2(c)) with triangular grid arrangement having inter-element spacings; $dx = 0.475\lambda_o$ and $dy = 0.538\lambda_o$, in H- and E-planes has been chosen in this work. The designed DTSA has been optimized in the array environment in HFSS using unit cell model, as shown in Figure 6(a), for the desired specifications mentioned previously. The simulated results from HFSS have been shown in Figures 6 and 7.

Figure 6 shows the active return loss of the centre element in the array environment with respect to scan angle variation, in E- and H-planes at centre frequency, f_0. Figures 7(a) and (b) show the simulated results of scanned beam patterns of uniformly illuminated 256 (16×16) elements antenna array including the element pattern showing the ability of array to scan over the desired scan volume mentioned previously in H- and E-planes, respectively. It has been shown in these figures that the planar array can scan over the desired scan volume of $\pm 60^\circ$ in H-plane and $\pm 50^\circ$ in E-plane. These studies have clearly established the suitability of the designed array element, DTSA, as a candidate for wide scanning active phased array.

5. FABRICATION AND MEASUREMENTS

DTSA has been designed to operate only in X-band as per the specified requirements. Figures 8(a) and (b) show the photograph of the rear and front views of the DTSA antenna element. A 16-element E-plane array with inter-element spacing; dx using the optimised DTSA as an array element was fabricated on two layers of Rogers RT Duroid 5880 substrate (with $\varepsilon_r = 2.2$ and thickness of $h_s = 31$ mils), shown as an inset in Figure 10. The two substrates were bonded together with the

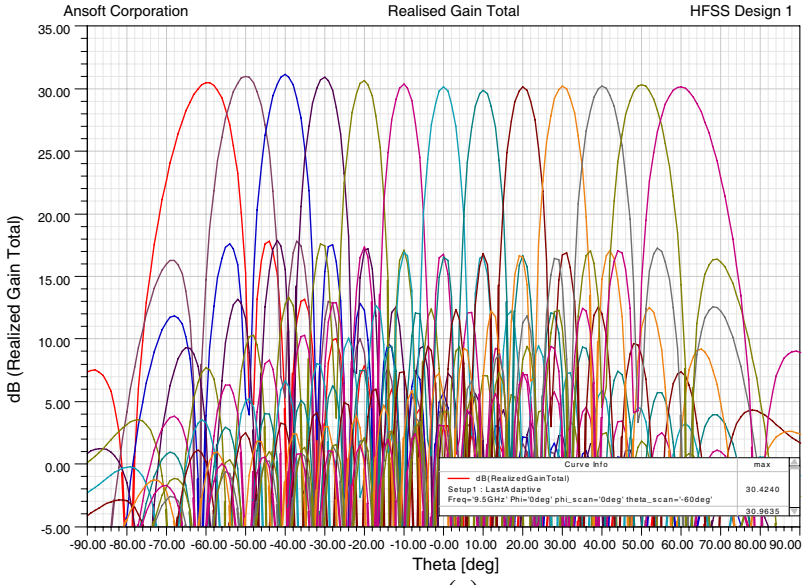

(a)

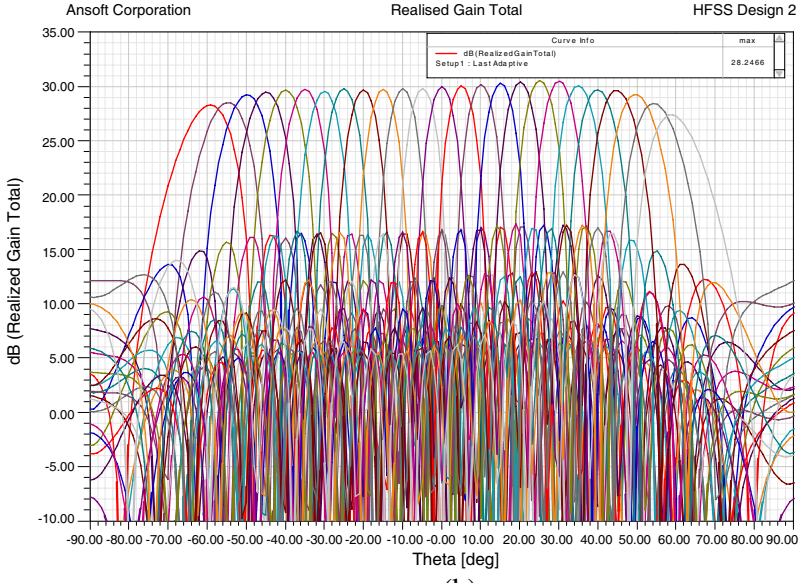

(b)

Figure 7. Simulated scan beam pattern of DTSA in (a) H-plane, (b) E-plane.

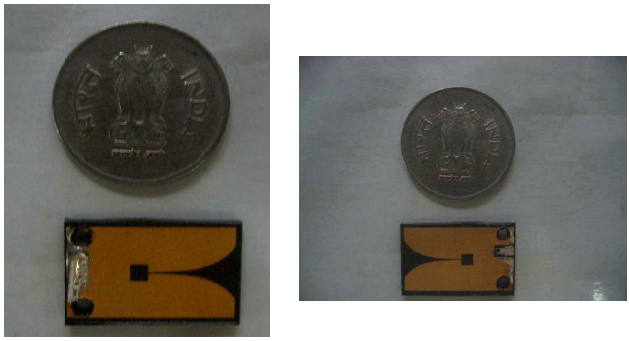

(a) (b)

Figure 8. Photograph of the fabricated DTSA in assembled manner being shown (a) rear view, (b) front view showing the CPW feed.

1–2 layers of Rogers 3001 bonding film [22] (5 mils in thickness) to glue them together without introducing any air gaps in between. Hence the overall thickness of antennas was approximately 70 mils.

After terminating all of the elements in matched loads except the centre element, i.e., 8th element in the E-plane linear array, the return loss and the E- and H-planes pattern measurements were carried out for evaluating the embedded element performance. Figure 9(a) shows the measured R.L. performance of the element acceptable over the desired band. Figure 9(b) shows the measured R.L. of DTSA in linear array with all elements except centre element terminated in $50\,\Omega$ matched loads clearly illustrating a value better than -10 dB over the desired frequency band. In the array environment, multiple resonances were observed due to the close proximity of array elements and probably due to the metallic base plate used for mounting the array elements. Measured mutual coupling was -18 dB for the immediate neighbouring elements to the centre element.

In Figures 10 and 11, measured radiation patterns in H- and E-planes of the 8th element at the centre frequency, f_0, with all other elements in linear array being terminated has been shown. A wide HPBW of 125 deg and 107 deg in H- and E-planes, respectively, has been achieved. Some reduction in HPBW and increase in cross-polarization has been observed due to the coupling from neighbouring array elements and the presence of metallic ground plane on which DTSA is mounted for pattern measurement and also due to some manufacturing tolerances while bonding two substrates together which led to the difference in the simulated and actual overall thickness of the substrate. The cross-polarization can be further improved by covering

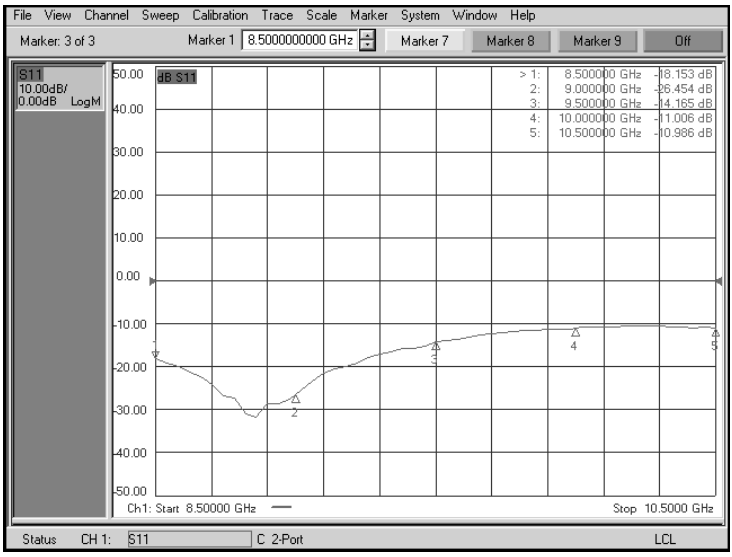

(a)

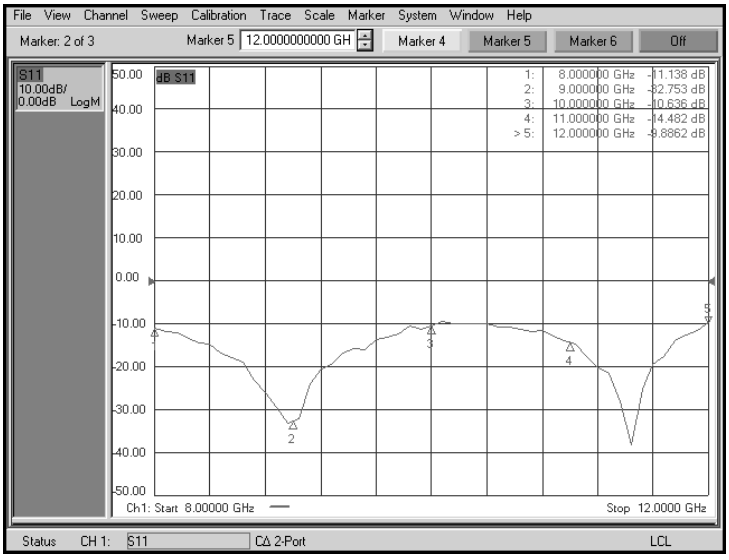

(b)

Figure 9. Measured return loss performance of DTSA in (a) isolated environment, (b) array environment.

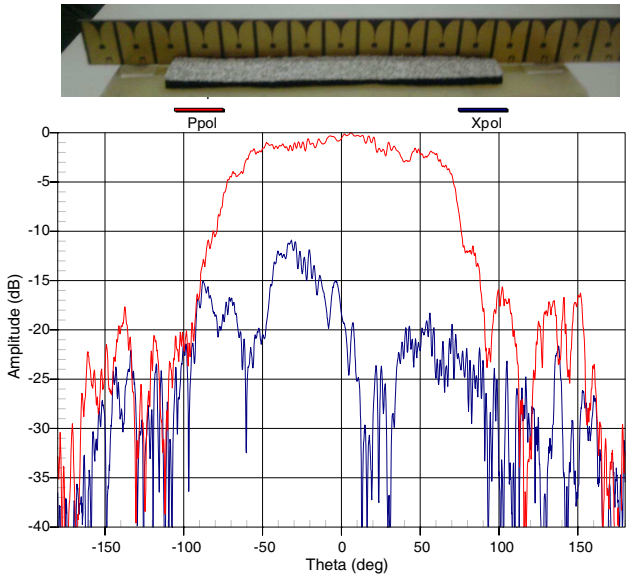

Figure 10. Measured H-plane radiation pattern plot of centre element of E-plane linear array (On top is shown photograph of the linear array).

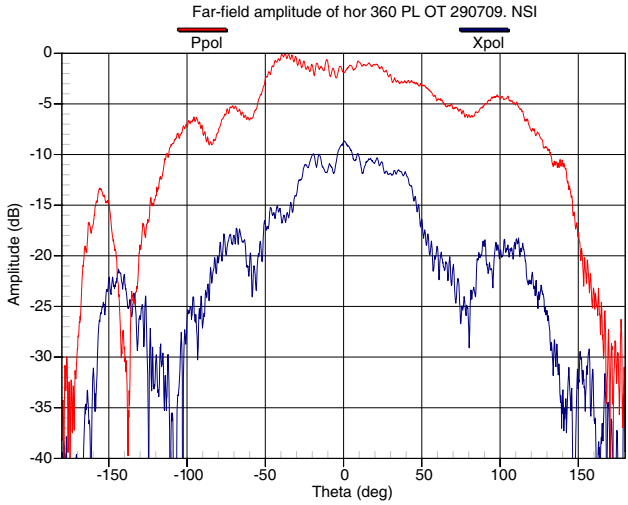

Figure 11. Measured E-plane radiation pattern plot of centre element of linear E-plane array.

ground plane with some absorbing material which may absorb the reflections from the ground planes. The measured gain observed was better than 4 dB over the frequency range.

Further efforts in developing and studying (16 × 16) elements planar array prototype as shown in Figure 2(c) are going on and may be communicated in future correspondences.

6. CONCLUSION

Design and development of a compact, low profile, wide band and wide beam CPW fed tapered slot antenna has been presented along with the measured results. The measured results have shown a wide beam width and a moderate gain of 4–7 dB over full X-band in array environment. The ripples in E-plane can be reduced by increasing the separation of flare from the mounting structure and by covering the ground with some absorbing material. This antenna is a promising candidate for the airborne active phased array radars and other similar applications.

ACKNOWLEDGMENT

The authors will like to acknowledge the support extended by Director, LRDE in carrying out the work. They would also like to thank the antenna measurement, drawing and fabrication divisions at LRDE for their support in realizing the structure.

REFERENCES

1. Skolnik, M. I., *Introduction to Radar Systems*, McGraw Hill Book Company, 1981.
2. Lacomme, P., J. P. Hardange, J. C. Marchais, and E. Normant, *Air and Spaceborne Radar Systems: An Introduction*, Scitech Publishing Inc., 2001.
3. Stimson, G. W., *Introduction to Airborne Radar*, Scietch Publishing Inc., 1998.
4. Hemmi, C., R. T. Dover, F. German, and A. Vespa, "Multifunction wide band array design," *IEEE Trans. Antennas Propag.*, Vol. 47, 425–431, Mar. 1999.
5. Axness, T. A., R. V. Coffman, B. A. Kopp, and K. W. O'Haver, "Shared aperture technology development," *Johns Hopkins APL Tech. Dig.*, Vol. 17, 1996.
6. Chang, K., *Encyclopaedia of RF and Microwave Engineering*, 3535–3546, John Wiley and Sons, 2006.

7. Balanis, C. A., *Modern Antenna Handbook*, John Wiley and Sons, 2008.
8. Amitay, N., V. Galindo, and C. P. Wu, *Theory and Analysis of Phased Array Antennas*, Wiley Interscience, 1972.
9. Visser, H. J., *Array and Phased Array Antenna Basics*, John Wiley and Sons, 2005.
10. Trifunovic, V. and B. Jokanovic, "Review of printed marchand and double baluns: characteristics and application," *IEEE Trans. Microwave Theory Tech.*, Vol. 42, 1454–1462, Aug. 1994.
11. Abbosh, A. M. and M. E. Bialkowski, "Compact directional antenna for ultra wideband microwave imaging system," *Microw. Opt. Tech. Letters*, Vol. 51, No. 12, 2898–2901, Dec. 2009.
12. Acharya, P. R., H. Ekstrom, S. S. Gearhart, S. Jacobsson, J. F. Johansson, E. L. Kollberg, and G. M. Rebeiz, "Tapered slotline antennas at 802 GHz," *IEEE Trans. Microwav. Theory Tech.*, Vol. 41, No. 10, Oct. 1993.
13. High Frequency Structure Simulator (HFSS), Ver. 11, Ansoft Corporation.
14. Ellgardt, A., "A scan blindness model for single-polarized tapered slot arrays in triangular grids," *IEEE Trans. Antennas Propag.*, Vol. 56, 2937–2942, Sep. 2008.
15. Shin, J. and D. H. Schaubert, "A parameter study of stripline-fed vivaldi notch antenna arrays," *IEEE Trans. Antennas Propag.*, Vol. 47, 879–886, 1999.
16. Schaubert, D. H., A. O. Boryssenko, and T. H. Chio, "Analysis of finite arrays of wideband tapered slot antennas," *URSI Gen. Assembly*, Maastricht, The Netherlands, 2002.
17. Schaubert, D. H. and T. H. Chio, "Wideband vivaldi arrays for large aperture antennas," *NFRA Int. Conf. Perspectives in Radio Astronomy: Technologies for Large Antenna Arrays*, 49–57, Dwindeloo, Netherlands, Apr. 1999.
18. Marchand, N., "Transmission line conversion," *Electronics*, Vol. 17, 142–145, 1944.
19. Knorr, J. B., "Slotline transitions," *IEEE Trans. Microwave Theory Tech.*, Vol. 22, 48–54, 1974.
20. Shafieha, J. H., J. Noorinia, and C. Ghobadi, "Probing the feed line parameters in vivaldi notch antennas," *Progress In Electromagnetics Research B*, Vol. 1, 237–252, 2008.
21. Itoh, T., et al., *Finite Element Software for Microwave Engineering*, Ch. 10, John Wiley and Sons, 1996.
22. High Frequency Laminates, Rogers Corporation, USA.